Ballistic deposition on deterministic fractals: Observation of discrete scale invariance

Claudio M. Horowitz,[1] Federico Romá,[2] and Ezequiel V. Albano[1]
[1]*Instituto de Investigaciones Fisicoquímicas Teóricas y Aplicadas (INIFTA), UNLP, CCT La Plata-CONICET, Sucursal 4, Casilla de Correo 16, (1900) La Plata, Argentina*
[2]*Centro Atómico Bariloche, 8400 S. C. de Bariloche, Río Negro, Argentina*
(Received 29 May 2008; published 16 December 2008)

The growth of ballistic aggregates on deterministic fractal substrates is studied by means of numerical simulations. First, we attempt the description of the evolving interface of the aggregates by applying the well-established Family-Vicsek dynamic scaling approach. Systematic deviations from that standard scaling law are observed, suggesting that significant scaling corrections have to be introduced in order to achieve a more accurate understanding of the behavior of the interface. Subsequently, we study the internal structure of the growing aggregates that can be rationalized in terms of the scaling behavior of frozen trees, i.e., structures inhibited for further growth, lying below the growing interface. It is shown that the rms height (h_s) and width (w_s) of the trees of size s obey power laws of the form $h_s \propto s^{\nu_\parallel}$ and $w_s \propto s^{\nu_\perp}$, respectively. Also, the tree-size distribution (n_s) behaves according to $n_s \sim s^{-\tau}$. Here, $\nu_\parallel$ and $\nu_\perp$ are the correlation length exponents in the directions parallel and perpendicular to the interface, respectively. Also, τ is a critical exponent. However, due to the interplay between the discrete scale invariance of the underlying fractal substrates and the dynamics of the growing process, all these power laws are modulated by logarithmic periodic oscillations. The fundamental scaling ratios, characteristic of these oscillations, can be linked to the (spatial) fundamental scaling ratio of the underlying fractal by means of relationships involving critical exponents. We argue that the interplay between the spatial discrete scale invariance of the fractal substrate and the dynamics of the physical process occurring in those media is a quite general phenomenon that leads to the observation of logarithmic-periodic modulations of physical observables.

DOI: 10.1103/PhysRevE.78.061118 PACS number(s): 02.50.−r, 68.35.Ct, 81.15.Aa

I. INTRODUCTION

The study, characterization, and understanding of growth processes that take place under far-from-equilibrium conditions are topics that have attracted great attention due to their relevance in many fields of science and technology [1–4]. Growing aggregates of biological origin (bacteria, fungi, tumors, etc.), the deposition of thin films, the growth of magnetic materials, alloys and polymers, among others, have recently become the subject of extensive studies [1,5–8]. Also, the dynamic evolution of interfaces is closely related to almost all growth processes [1]. The characterization of the properties of interfaces has achieved considerable progress during the last two decades, mostly due to the success of the concepts of the dynamic scaling theory developed by Family and Vicsek [9,10], which allows a comprehensive description of interfaces in terms of universality classes that group systems described by the same set of physically meaningful exponents.

In order to provide a more complete description of growing aggregates, it is desirable not only to focus on the properties of the evolving interface, but also to attempt the simultaneous characterization of bulk properties. In fact, in some cases, growing processes lead to the formation of porous materials that inherently have very interesting physical and chemical properties with many potential practical applications.

Within this broad context, ballistic deposition (BD), which was originally proposed by Vold [11] as a model for the description of sedimentary rock formation, has become an archetypical system for the study of growing aggregates [1]. BD aggregates are characterized by a porous structure in the bulk and a rough evolving interface. The interface roughness of BD has been extensively studied by means of computer simulations and analytical approaches in connection to the Kardar-Parisi-Zhang (KPZ) theory [1,12].

In spite of the considerable effort devoted to understanding growing aggregates in Euclidean substrates [1–4], to the best of our knowledge little attention has been drawn to the study of deposition models on fractal media. It should be expected that the interplay between the self-similarity of the substrates and the growing mechanisms would lead to the formation of interesting and complex porous (bulk) structures. Also, the fractality of the substrate would affect the self-affine nature of the growing interface. So, it would not be surprising to find nonvanishing scaling corrections to the well-established phenomenological dynamic approach of Family-Vicsek [1,9,10]. In fact, in some pioneering works [13,14] and in more recent ones [15–17] it has been shown that the power-law behavior of some observables becomes modulated by logarithmic oscillations due to the effect of the underlying lattice structure. Also, in recent years two interesting books have been published where this issue is addressed [18,19].

Within this context, the aim of this paper is to study the scaling behavior of the BD model on deterministic fractal substrates. The study is based on Monte Carlo numerical simulations analyzed by means of the Family-Vicsek phenomenological scaling approach [9,10] and on extensive numerical investigations of the scaling behavior of the internal structures of the growing system [20–25]. For this purpose the manuscript is organized as follows: firstly, in Sec. II we provide a brief theoretical background on the scaling behav-

ior of growing aggregates. The fractal substrates used for the growth of BD aggregates and the concepts of space and time discrete scale invariance are described and discussed in Sec. III. Subsequently, in Sec. IV, we describe the BD model on fractal media, as well as the determination of the internal structure of the aggregates in terms of frozen and growing trees. The results obtained by applying the standard dynamic scaling approach to the data are presented and discussed in Sec. V, while the analysis of the data of the internal structure of the aggregates is performed in Sec. VI. Finally, our conclusions are stated in Sec. VII.

II. BRIEF THEORETICAL BACKGROUND

Models aimed to describe growing aggregates may be defined and studied by means of both continuous approaches, which involve the formulation of analytical equations, and discrete lattice models, which consider the deposition of individual particles. A discrete model is defined by means of a set of deposition rules that provides a detailed microscopic description of the evolution of the aggregate. In these discrete models, the growing interface of the aggregate is described by a discrete set $h(i,t)$, which represents the height of site i at time t. The interface then has L^d sites, where L is the linear size and d is the dimensionality of the substrate (as usual, d is assumed to be an integer).

The dynamic evolution of the aggregate interface is characterized through the scaling behavior of the interface width $W(L,t)$, given by

$$W(L,t) \equiv \sqrt{1/L^d \sum_{i=1}^{L^d} [h(i,t) - \langle h(t) \rangle]^2}. \tag{1}$$

For this purpose, the Family-Vicsek phenomenological scaling approach [9,10], which has proved to be very successful, can be written as

$$W(L,t) = L^{\alpha} W^*(t/L^z), \tag{2}$$

where W^* is a scaling function. In fact, it may be expected that $W(L,t)$ will show the spatiotemporal scaling behavior given by [9,10]: $W \propto L^{\alpha}$ for $t \gg t_c$ and $W(t) \propto t^{\beta}$ for $t \ll t_c$, where $t_c \propto L^z$ is the crossover time between these two regimes. The scaling exponents α, β, and $z=\alpha/\beta$ are called roughness, growth, and dynamic exponents, respectively. Also, different models can be grouped into universality classes when they share the same scaling exponents.

An alternative method that can also be used for the characterization of interfaces is related to the description of the internal structure of the growing system. This approach is based on the fact that any growing system can effectively be rationalized on the basis of a treeing process, i.e., any growing structure can be thought of as the superposition of individual trees [20–23,26]. Those trees that spread out incorporating additional growing centers, e.g., capturing particles, developing new branches, are said to be alive. In contrast, other trees that may stop growing due to shadowing by surrounding growing trees are termed dead trees. The structure of dead trees remains frozen because it cannot be modified by any further growth. It is well known that for growing aggregates on substrates having integer dimension, the rms height (h_s) and the rms width (w_s) of dead trees of size s (s is the number of particles belonging to the tree) obey simple power laws given by

$$h_s \propto s^{\nu_{\parallel}}, \tag{3}$$

and

$$w_s \propto s^{\nu_{\perp}}, \tag{4}$$

where $\nu_{\parallel}$ and $\nu_{\perp}$ are the correlation length exponents parallel and perpendicular to the main growing direction of the aggregate [20–23,25,26], respectively.

By assuming both the proportionality between the correlation length perpendicular to the main growing direction and w_s, as well as $h_s \propto t$, one has that the dynamic exponent $z=\alpha/\beta$ is given by [27]

$$z = \nu_{\parallel}/\nu_{\perp}. \tag{5}$$

Furthermore, one also expects that during the competition among trees along the evolution of the aggregate, the existence of large neighboring trees may inhibit the growing of smaller ones. This competing process ultimately leads to the death of some trees that become frozen within the underlying aggregate. These prevailing large trees continue the competition within more distant trees in a dynamic process. Since this situation takes place on all scales, it is reasonable to expect that the tree-size distribution (n_s) should also exhibit a power-law behavior, so that [20–23,26,27]

$$n_s \sim s^{-\tau}, \tag{6}$$

where τ is an exponent.

III. FRACTAL SUBSTRATES AND DISCRETE SCALE INVARIANCE

In the present paper we used Sierpinski carpets (SC's) as substrates for the growth of ballistic aggregates. In fact, SC's provide generic models for the building of both deterministic and nondeterministic fractals. In order to generate a SC embedded in $d=2$ dimensions, one proceeds as follows: a square is divided into l^2 subsquares, and then (l^2-N_{occ}) subsquares are deleted from the initial square (N_{occ} is the number of occupied subsquares). This process is iterated in the remaining subsquares k times, where k accounts for the number of different generations. If the deleted subsquares are chosen in the same way in all iterations, the resulting fractal is deterministic, but if the deleted subsquares are selected at random, one generates a nondeterministic fractal. The mathematical fractal, obtained in the limit $k \to \infty$, is generically called $\mathrm{SC}_x(l,N_{occ})$. Also, the fractal associated with a finite number of segmentation steps is denoted by $\mathrm{SC}_x(l,N_{occ},k)$. In both cases the index x refers to the topological features of the generating cell $[\mathrm{SC}_x(l,N_{occ},1)]$. The size of the lattice, where the finite fractal is embedded, then is $L=l^k$.

For deposition models grown in integer-dimensional substrates one always has that all fragments or parts of the aggregate are connected to each other through paths of nearest-neighbor occupied sites. So, it is no longer possible to have

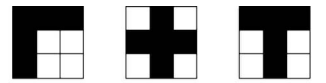

FIG. 1. Sketches of the three different generating cells used to grow ballistic aggregates by keeping $l=3$ and $N_{occ}=5$.

isolated fragments of the aggregate on the substrate. On the other hand, for some fractal substrates with noninteger fractal dimension, it could be possible to observe the formation of isolated fragments of the aggregate, and consequently, in order to avoid this shortcoming, one has to carefully select suitable substrates. So, this point is essential for the choice of the fractals that can be used in order to study ballistic deposition on this kind of substrate. Accordingly, in this paper we use deterministic fractal substrates generated by taking $l=3$ and $N_{occ}=5$, and in order to prevent the fragmentation of the aggregates, as mentioned above, and to account for the usual requirement of periodic boundary conditions, one ends up with only three generating cells, as shown in Fig. 1.

Let us now discuss the concepts of fractal dimensionality and discrete scale invariance associated with the SC's used. The fractal dimension d_f characterizes the dependence of the mass $M(L)$ (or equivalently, the number of occupied sites of the fractal) as a function of the linear size L of the system, so that if we now consider an amplification of the system of size bL, one has

$$M(bL) = b^{d_f} M(L), \tag{7}$$

which yields the following solution:

$$M(L) = BL^{d_f}, \tag{8}$$

where B is a constant and d_f is a noninteger dimension known, after Mandelbrot, as the fractal dimension. By applying Eq. (7) to the carpets $\mathrm{SC}_x(l,N_{occ},k)$ one gets $d_f = \ln(N_{occ})/\ln(l)$, which leads to $d_f = \ln(5)/\ln(3) \simeq 1.465$ for the carpets shown in Fig. 1 with $l=3$ and $N_{occ}=5$.

In general, the factor b in Eq. (7) could be an arbitrary real number, leading to *continuous* scale invariance. However, deterministic fractals exhibit *discrete* scale invariance (DSI) [28], which is a weak kind of scale invariance such that b is no longer an arbitrary real number, but it can only take specific discrete values of the form $b_n=(b_1)^n$, where b_1 is a fundamental scaling ratio. Then, for the case of DSI, the solution of Eq. (7) yields

$$M(L) = L^{d_f} F\left(\frac{\ln(L)}{\ln(b_1)}\right), \tag{9}$$

where F is a periodic function of period one. Notice that for the $\mathrm{SC}_x(l,N_{occ},k)$ one has that $b_1=l$. The measurement of soft oscillations in spatial domain [28] is a signature of spatial DSI.

Very recently one of us found evidence of discrete scale invariance in the time domain by measuring the relaxation of the magnetization in the Ising model on Sierpinski carpets [15,16]. Subsequently, it has been conjectured that physical processes characterized by an observable $O(t)$, occurring in fractal media with DSI, and that develop a monotonically increasing time-dependent characteristic length $\xi(t)$, may also exhibit time DSI [17]. In fact, by assuming

$$\xi \propto t^{1/z_D}, \tag{10}$$

where z_D is a dynamic exponent, it can be shown that $O(t)$ has to obey time DSI according to [17]

$$O(t) = Ct^{\gamma/z_D} F\left(\phi + \frac{\ln(t)}{\ln(b_1^{z_D})}\right), \tag{11}$$

where C and ϕ are constants, and γ is the relevant exponent in the expected power-law behavior of the observable $O(t)$. So, the conjecture given by Eq. (11) implies the existence of a logarithmic periodic modulation of time observables characterized by a time-scaling ratio T given by

$$T = b_1^{z_D} \tag{12}$$

[see also Eq. (9)]. It is worth mentioning that in the case of growth models, Eq. (10) can be identified, e.g., with the time development of the correlation length along the direction parallel to the interface given by $\xi_{\parallel} \propto t^{1/z}$.

As follows from Fig. 1, in this work only fractals with finite ramification order [30] are used. A finite ramification implies that the fractal structure has weak points, where only a finite number of links connect two parts of arbitrary size together.

IV. BD MODEL ON FRACTAL SUBSTRATES AND DEFINITION OF ITS INTERNAL STRUCTURE

The lattice version of BD is simple to describe: particles fall vertically onto the substrate from a random position above the surface. When a particle reaches the surface, it sticks on the first site encountered that is a nearest neighbor of an already deposited particle. Due to this constraint the growth of an interface essentially parallel to the substrate is observed. For substrates of integer dimension, the BD model can be described by the KPZ equation [1,12], namely,

$$\frac{\partial h(\mathbf{x},t)}{\partial t} = \mathcal{F} + \nu_0 \nabla^2 h(\mathbf{x},t) + \frac{\lambda}{2}[\nabla h(\mathbf{x},t)]^2 + \eta(\mathbf{x},t). \tag{13}$$

In this equation the nonlinear term represents the lateral growth or the appearance of a driven force, ν_0 accounts for the effective surface tension, $\mathcal{F}$ is the flux of incoming particles, and $\eta(\mathbf{x},t)$ is a Gaussian noise with zero configurational average. In $d=1$ dimension, Eq. (13) can be solved exactly and the resulting exponents are $z=3/2$, $\alpha=1/2$, and $\beta=1/3$. For $d=2$ dimensions, one still lacks an analytical solution, but according to numerical simulations one has estimations of the exponents given by $\alpha \sim 0.40$ and $\beta \sim 0.24$ [29].

In order to describe the internal structure of BD aggregates, one considers that trees are formed by assuming that any newly deposited particle belongs to the same tree as that of the nearest-neighbor particle where it is attached [24]. Also, if the deposited particle has more than one nearest neighbor belonging to different trees, one of them is selected at random and the particle is incorporated into that tree. Relevant exponents [see Eqs. (3), (4), and (6)] have already been

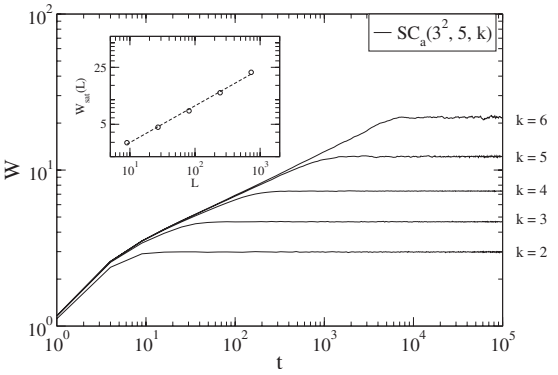

FIG. 2. Log-log plots of the interface width (W) versus time for the BD model on $SC_a(3^2,5,k)$ with $k=2-6$. The inset shows a log-log plot of $W_{sat}(L)$ versus L. The dotted line with slope 0.47 corresponds to the best fit of the data.

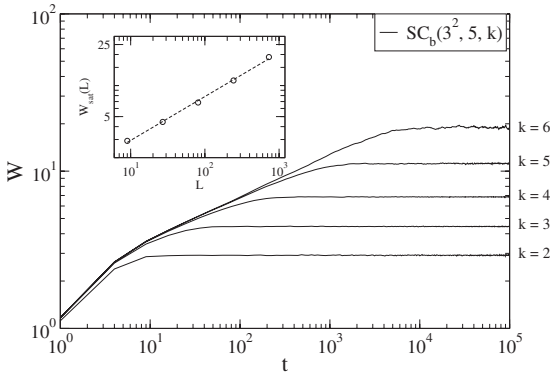

FIG. 3. Log-log plots of the interface width (W) versus time for the BD model on $SC_b(3^2,5,k)$ with $k=2-6$. The inset shows a log-log plot of $W_{sat}(L)$ versus L. The dashed line with slope 0.44 corresponds to the best fit of the data.

determined yielding $\nu_{\parallel}=0.60(1)$, $\nu_{\perp}=0.40(1)$, and $\tau=1.40(1)$ in $d=1$ dimension, and $\nu_{\parallel}=0.45(1)$, $\nu_{\perp}=0.29(1)$, and $\tau=1.57(1)$ in $d=2$ dimensions (see, e.g., [24], and references therein).

On the other hand, for BD growth on fractal substrates, particles are deposited randomly on *occupied sites of the fractal only* by following the rules described above for the case of integer-dimensional substrates. Also, the building procedure employed to determine the trees used for the description of the internal structure of the whole aggregate is independent of the substrate.

For the purpose of a numerical simulation, the Monte Carlo time step (MCS) involves the deposition of L^{d_f} particles.

V. APPLICATION OF THE FAMILY-VICSEK PHENOMENOLOGICAL DYNAMIC SCALING APPROACH

Figure 2 shows log-log plots of W versus t obtained for the BD model on fractal substrates obtained by using the generating cell $SC_a(3,5,1)$. For short times, say $t<3$ MCS, the random growth of the interface is observed because the random deposition (RD) process dominates. At this stage, correlations have not been developed yet and one has that, according to Eq. (2), $W(t)\propto t^{\beta_{RD}}$, with $\beta_{RD}=1/2$, holds. During an intermediate time regime, say 3 MCS $<t<t_c$, correlations develop since the BD process now prevails, leading to the typical growth regime $W(t)\propto t^{\beta_{BD}}$ [see also Eq. (2)]. At a later stage, for $t>t_c$, correlations can no longer develop due to the geometrical constraint of the lattice size, and the saturation regime $[W_{sat}(L)\propto L^{\alpha_{BD}}]$ is observed, as expected from Eq. (2). Here, $t_c\propto L^z$ is the crossover time between the growing and the saturation regimes of the interface width.

In order to obtain the roughness, growth, and dynamic exponents, we followed the standard procedure [1], e.g., the inset in Fig. 2 shows a log-log plot of $W_{sat}(L)$ versus L. Here, a slight but noticeable systematic upward deviation of the data is observed. However, an effective exponent (α) can be determined and the best fit of the data yields $\alpha=0.47\pm0.04$. Also, we determined $\beta=0.28\pm0.03$ and $z=1.56\pm0.05$ for the BD model on the fractal substrate obtained by using the $SC_a(3,5,1)$ generating cell.

Figures 3 and 4 show log-log plots of W versus t obtained for the BD model on fractal substrates built up by using the generating cells $SC_b(3,5,1)$ and $SC_c(3,5,1)$, respectively. Again, the standard procedure was attempted in order to determine the roughness, growth, and dynamic exponents. Accordingly, the insets in Figs. 3 and 4 show log-log plots of $W_{sat}(L)$ versus L. For the case of the $SC_b(3,5,1)$, again, a noticeable systematic upward deviation of the data is observed, but an effective exponent (α) can be determined, yielding $\alpha=0.44\pm0.04$. Also, we determined $\beta=0.26\pm0.03$ and $z=1.55\pm0.05$. On the other hand, for the $SC_c(3,5,1)$ we observed strong systematic deviations of the data that prevent the evaluation of the exponents. These results strongly suggest that in the case of aggregates grown on fractals generated by $SC_c(3,5,1)$ either the finite-size effects are very important and one has to introduce important scaling corrections to the standard Family-Vicsek approach, or (instead of not being able to identify two competing processes leading to the formation of the aggregate) eventually the onset of a crossover effect is present. The understanding or clarification of which one of the two possibilities may be true is a very difficult task, which deserves further work, and is beyond the scope of the present paper.

Anyway, the obtained effective exponents are almost the same (within error bars) for both the $SC_a(3,5,1)$ and the

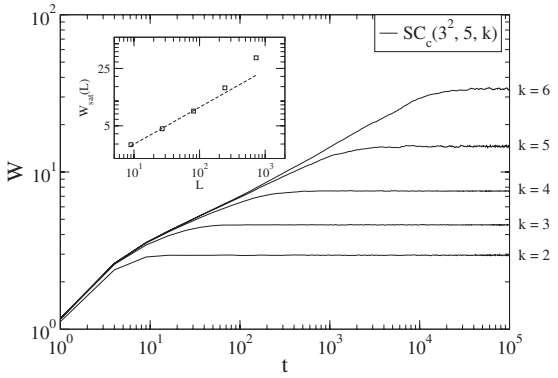

FIG. 4. Log-log plots of the interface width (W) versus time for the BD model on $SC_c(3^2,5,k)$ with $k=2-6$. The inset shows a log-log plot of $W_{sat}(L)$ versus L. The dashed line with slope 0.48 has been drawn for the sake of comparison.

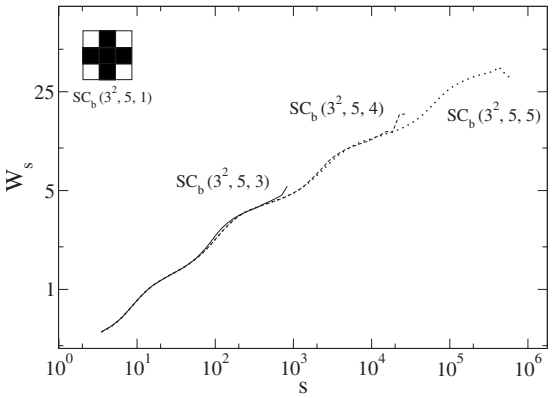

FIG. 5. Log-log plots of rms width of the trees as a function of the tree size s for the BD model on $SC_b(3,5,k)$ substrates ($k=3,4,5$).

$SC_b(3,5,1)$, namely, $\alpha \approx 0.46$, $\beta \approx 0.27$, and $z \approx 1.55$. It is worth mentioning that these exponents nicely interpolate between the exact values corresponding to $d=1$ and the best estimates reported for $d=2$, namely, $0.24(d=2) < \beta \approx 0.27 < 1/3(d=1)$, $0.40(d=2) < \alpha \approx 0.46 < 1/2(d=1)$, and $1.67(d=2) > z \approx 1.55 > 3/2(d=1)$.

VI. CHARACTERIZATION OF THE INTERNAL STRUCTURE OF THE AGGREGATES

The dependence of the rms width and rms height of the trees forming the aggregates on the tree size s, for the cases of the $SC_b(3,5,k)$ substrates ($k=3,4,5$), is shown in log-log plots in Figs. 5 and 6, respectively. For the growth of the BD model on nonfractal substrates it is known that the power laws given by Eqs. (3) and (4) hold [24], but in the case of fractal media, one also clearly observes soft oscillations with a logarithmic period, which modulate the power laws. Figures 5 and 6 also show a direct relationship between the number of observed oscillations and the generation (k) of the Sierpinski carpets used as substrates.

Figure 7 shows log-log plots of the tree-size distribution functions corresponding to the BD model grown on $SC_b(3,5,k)$ substrates ($k=2,3,4,5$). Again, for the BD model on nonfractal substrates the power law given by Eq. (6) holds, but when a fractal carpet is used as substrate, a soft oscillation with a logarithmic period modulates the power-law behavior. Also, there is a one to one relationship between the number of observed oscillations and the number of generations of the carpet.

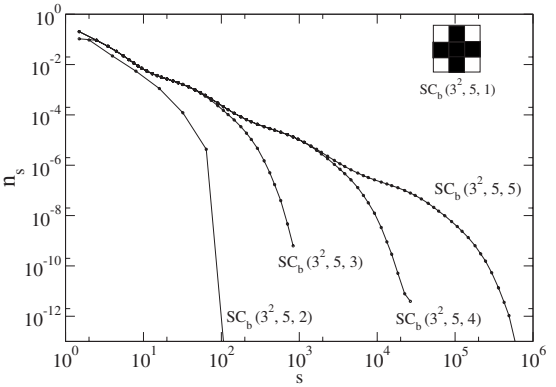

FIG. 7. Log-log plots of the tree-size distribution corresponding to the BD model on $SC_b(3,5,k)$ substrates ($k=2,3,4,5$).

After a systematic study, we found that the rms width, the rms height, and the tree-size distribution for BD aggregates grown on different deterministic fractal substrates, generated by $l=3$ and $N_{occ}=5$, exhibit a quite similar behavior, namely, soft oscillations with a logarithmic period, which modulate the expected power laws. Figures 8–10, show log-log plots of the rms width, the rms height, and the tree-size distribution, obtained for these fractal substrates, respectively. Table I summarizes the exponents obtained by fitting the modulated power laws describing the properties of the internal structure of the aggregates. Also, data corresponding to the exponent z obtained by means of the Family-Vicsek dynamic scaling approach have been included for the sake of comparison. The values of the exponents $Y \equiv \nu_{\parallel}$, $\nu_{\perp}$, and τ, have been obtained by fitting the data with the function

$$\frac{d\ln(X)}{d\ln(s)} = Y + \sum_{n=1}^{N} b_n \cos[n\omega \ln(s) + \xi_n], \tag{14}$$

where $X \equiv h_s$, w_s, and n_s, respectively [31]. Here, b_n and ξ_n are constants. When the fit is performed by taking $N>1$, the

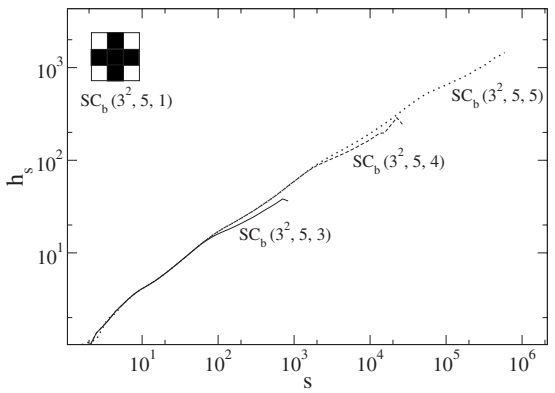

FIG. 6. Log-log plots of rms height of the trees as a function of the tree size s for the BD model on $SC_b(3,5,k)$ substrates ($k=3,4,5$).

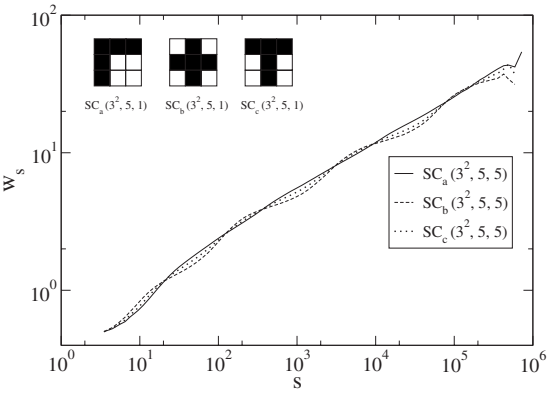

FIG. 8. Log-log plots of rms width of the trees as a function of the tree size s for the BD model on $SC_x(3,5,5)$ substrates ($x=a,b,c$).

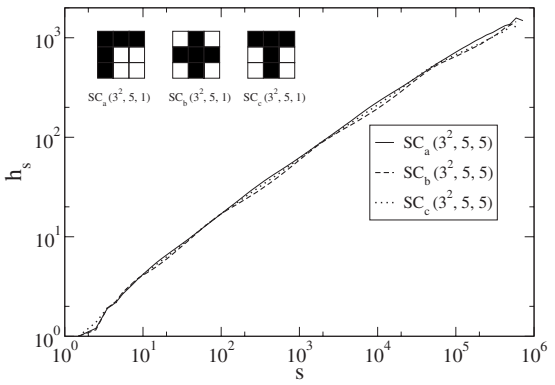

FIG. 9. Log-log plots of rms height of the trees as a function of the tree size s for the BD model on $SC_x(3,5,5)$ substrates ($x=a,b,c$).

presence of higher harmonics to the fundamental frequency is considered. So, the values of the exponents obtained by using $N=1$ could be improved [31]. However, when we considered higher harmonics, in spite of the fact that typically we have $b_2/b_1 \sim 0.2$, the values of the exponents obtained by fitting the data with $N=1$, and 2, are almost indistinguishable (within errors bars).

In order to rationalize our findings, let us discuss the soft oscillations observed in the rms width mentioned above. Here, we can identify two logarithmic periods, one for the size of the trees (λ_s) and the other for the rms width (λ_{w_s}), as is schematically shown in Fig. 11. These periods become evident by calculating the derivative of $\ln(w_s)$ with respect to $\ln(s)$, and the derivative of $\ln(s)$ with respect to $\ln(w_s)$, as shown in Fig. 12 for the case of the $SC_b(3,5,5)$ substrate. Also, it is worth mentioning that by following the same procedure, we can identify one logarithmic period for the rms height (λ_{h_s}) and another one for the size distribution (λ_{n_s}). Furthermore, as mentioned above, there is a one to one relationship between the number of observed oscillations and the generations of the carpets. So, as all measurements share the same range of values of s, the period of the oscillation observed for the size of the trees (λ_s), when k tends towards infinity, has to be the same for all observables, namely, the rms width, the rms height, and the tree-size distribution.

Now, based on both the already discussed results and Eq. (4), we conjecture that for the case of a fractal substrate and

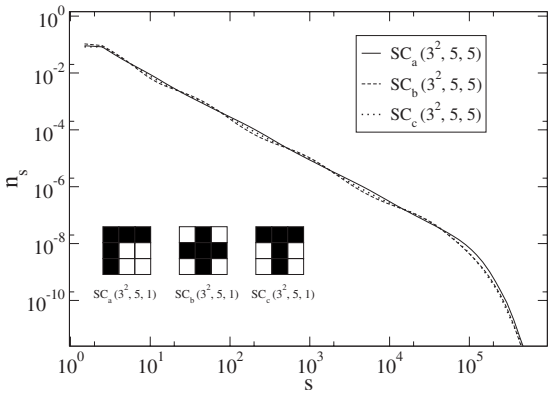

FIG. 10. Log-log plots of the tree-size distribution corresponding to the BD model on $SC_x(3,5,5)$ substrates ($x=a,b,c$).

TABLE I. List of exponents describing the properties of the internal structure of ballistic aggregates on different fractals. The exponent z (column 5) is obtained by using Eq. (5) and the values of $\nu_\perp$ and $\nu_\parallel$ are listed in columns 2 and 3, respectively. Also, the exponent z (column 6) is evaluated by using data obtained by applying the Family-Vicsek dynamic scaling [Eq. (2)].

Generating cell	$\nu_\perp$	$\nu_\parallel$	τ	$z=\nu_\parallel/\nu_\perp$	$z=\alpha/\beta$
$SC_a(3,5,1)$	0.34(1)	0.54(1)	1.48(1)	1.59(6)	1.56(5)
$SC_b(3,5,1)$	0.34(1)	0.55(1)	1.48(1)	1.60(6)	1.55(5)
$SC_c(3,5,1)$	0.35(1)	0.56(1)	1.48(5)	1.61(6)	

in the limit $k \to \infty$, the derivative of $\ln(w_s)$ with respect to $\ln(s)$ is a periodic function (with a logarithmic period) that modulates a constant value. So, the conjecture can be written as

$$\frac{\partial \ln(w_s)}{\partial \ln(s)} = \nu_\perp + \zeta[\ln(s)], \tag{15}$$

where $\zeta(x)$ is a periodic function. By integration of Eq. (15) it follows that

$$w_s = A s^{\nu_\perp} \exp^{\zeta^*[\ln(s)]}, \tag{16}$$

where A is a constant and $\zeta(x)^*$ is a periodic function such that $\partial\zeta^*[\ln(s)]/\partial \ln(s) = \zeta[\ln(s)]$.

Let us now take two tree sizes, s_a and s_b, separated by a period λ_s (on a logarithmic scale), as shown in the horizontal axis of Fig. 11. Also, their corresponding rms widths, called w_a and w_b, respectively, are separated on a logarithmic scale by a period λ_{w_s} (see Fig. 11). Then, by assuming that Eq. (16) holds, it can be found that

$$\lambda_{w_s} = \nu_\perp \lambda_s. \tag{17}$$

The existence of a logarithmic period in the rms width of the trees (λ_{w_s}) can be understood due to the fact that each tree can only spread over the fractal and, consequently, the rms width of the trees is constrained by the geometrical fea-

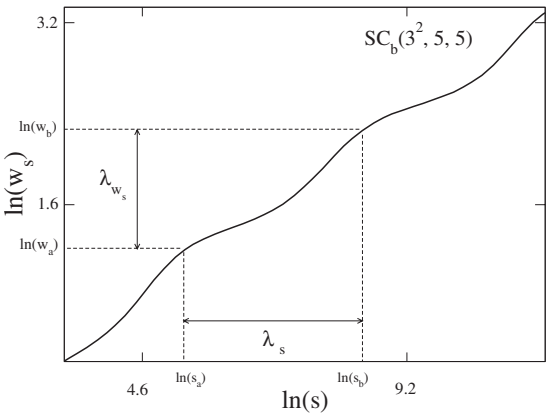

FIG. 11. Schematic view of the dependence of the rms width of the trees (w_s) versus the tree size (s), showing both the logarithmic period of the size of the trees (λ_s), and the logarithmic period of the rms width (λ_{w_s}).

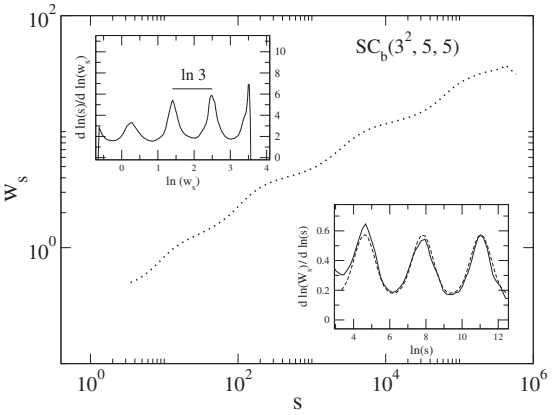

FIG. 12. Log-log plots of the rms width of the trees as a function of the tree size s as obtained for ballistic aggregates on $SC_b(3^2,5,5)$ substrates. The derivative of $\ln(w_s)$ with respect to $\ln(s)$ is shown in the inset placed at the right-hand side, while the derivative of $\ln(s)$ with respect to $\ln(w_s)$ is shown in the inset placed on the left-hand side. The dashed line in the inset placed on the right-hand side corresponds to the best fit of the data using Eq. (14).

tures of the underlying structure. In the case of a deterministic Siernspisky carpet, that structure is constructed by the iteration of a generating cell, so that the topological details of the generating cell are present in all of the sample. In our simulations, a generating cell of side $l=3$ leads to the occurrence of discrete scale invariance, such that the underlying structures are self-similar only at scales of size l^n, where n is an integer. Based on theses concepts, it is expected that $\lambda_{w_s}=\ln(3)$. In order to check this statement, in the inset shown on the left-hand side of Fig. 12 we have drawn a line of size ln(3), which nicely fits the logarithmic period of the oscillation of the rms width. This result has also been carefully checked for all the studied cases by measuring the peak-to-peak distance of the modulating oscillations. This finding leads us to conjecture that, for aggregate grown on deterministic fractal substrates generated by a generating cell $SC_x(l,N_{occ},1)$, the logarithmic period in the rms width of the trees should obey the following relationship:

$$\lambda_{w_s}=\ln(l). \tag{18}$$

Equation (18) reflects the fact that the size of the trees in the direction parallel to the substrate exhibits spatial discrete scale invariance with the same fundamental scaling ratio as that of the underlying fractal, namely, $b_1=l$ [see also Eq. (9)].

In order to check this conjecture, Fig. 13 shows a log-log plot of the rms width as a function of the tree size s for the case of an $SC_b(2,3,8)$ substrate. In this case, the size of the generating cell is $l=2$, so according to the conjecture we expect $\lambda_{w_s}=\ln(2)$. The inset in Fig. 13 shows the derivative of $\ln(s)$ with respect to $\ln(w_s)$, and a line of size ln(2), which nicely fits the value expected for λ_{w_s}, has been drawn.

In order to understand the oscillatory modulation of the power laws observed in the rms height of the trees, we followed the same method already discussed for the case of the rms width. Figure 14 shows the rms height as a function of

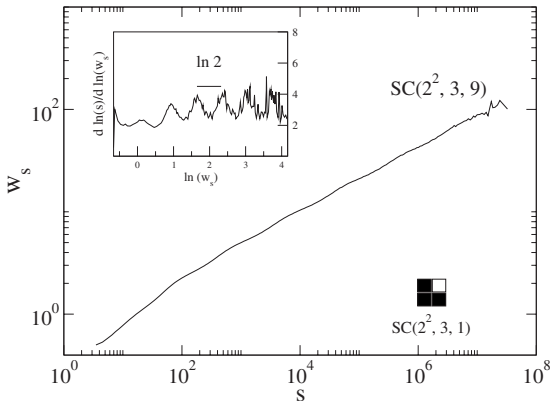

FIG. 13. Log-log plots of the rms width as a function of the tree size s as obtained for the $SC_b(2,3,9)$ substrate. The derivative of $\ln(s)$ with respect to $\ln(w_s)$ is shown in the inset.

the tree size s, as obtained for the $SC_b(3,5,5)$ substrate. Also, both the derivative of $\ln(h_s)$ with respect to $\ln(s)$ and the derivative of $\ln(s)$ with respect to $\ln(h_s)$ are shown in the insets placed on the lower right-hand and the upper left-hand sides of Fig. 14, respectively.

So, based on Eq. (3) and the obtained results, we now conjecture that

$$\frac{\partial \ln(h_s)}{\partial \ln(s)}=\nu_{\|}+\eta[\ln(s)], \tag{19}$$

where $\eta(x)$ is a periodic function. Then, after integration one gets

$$h_s=Bs^{\nu_{\|}}\exp^{\eta^*[\ln(s)]}, \tag{20}$$

where B is a constant and $\eta(x)^*$ is a periodic function such that $\partial\eta^*[\ln(s)]/\partial\ln(s)=\eta[\ln(s)]$.

By using Eq. (20) and following the method already applied to the case of the rms width, it can also be found that

$$\lambda_{h_s}=\nu_{\|}\lambda_s. \tag{21}$$

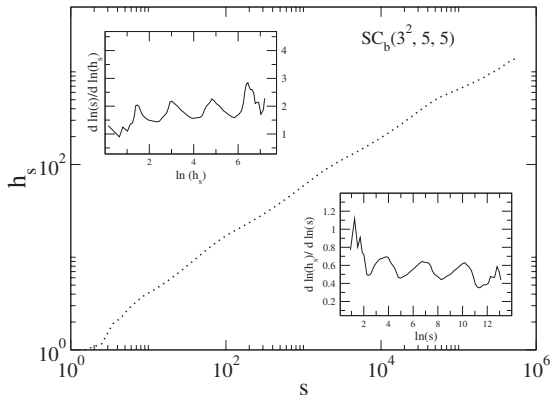

FIG. 14. Log-log plots of the rms height as a function of the tree size s as obtained for the $SC_b(3,5,5)$ substrate. The derivative of $\ln(h_s)$ with respect to $\ln(s)$ is shown in the inset placed on the right, and the derivative of the $\ln(s)$ with respect to $\ln(h_s)$ is shown in the inset placed on the left.

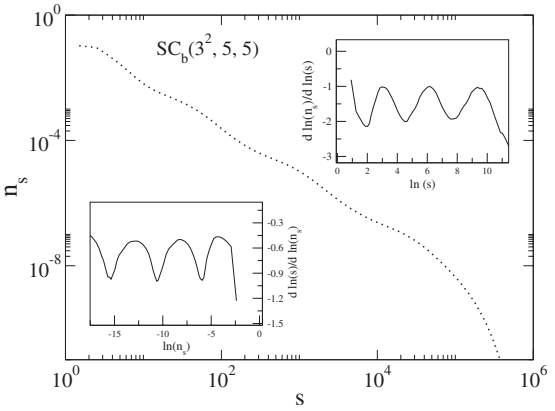

FIG. 15. Log-log plot of the tree-size distribution as obtained for the $SC_b(3,5,5)$ substrate. The derivative of $\ln(n_s)$ with respect to $\ln(s)$ is shown in the inset placed on the right, and the derivative of $\ln(s)$ with respect to $\ln(n_s)$ is shown in the inset placed on the left.

Then, by using Eqs. (17), (18), and (21) one obtains

$$\lambda_{h_s} = \frac{\nu_\parallel}{\nu_\perp} \ln(3) = z \ln(3) = z \ln(l) = z\lambda_{ws}, \tag{22}$$

where Eq. (5) has also been used. Let us now recall that, according to our conjecture given by Eq. (11), it should be expected that the rms high of the trees, which is an observable that evolves along the growing (time) direction, will be coupled to the space discrete scale invariance of the underlying fractal, then exhibiting time discrete scale invariance. In fact, the coupling is nicely reflected by Eq. (22), which is the realization of Eq. (12), with $T=\exp(\lambda_{h_s})$ being the fundamental time-scaling ratio.

Finally, the same procedure can be applied to understand the oscillation observed around the power laws of the size distribution. In fact, Fig. 15 shows the tree-size distribution function for the $SC_b(3,5,5)$ substrate. The derivative of $\ln(n_s)$ with respect to $\ln(s)$ is shown in the inset placed on the left-hand side, while the derivative of $\ln(s)$ with respect to $\ln(n_s)$ is shown in the inset placed on the right-hand side.

Based on the obtained results, now we conjecture that in the case of a fractal substrate where k tends towards infinity, the logarithmic derivative of the size distribution with respect to $\ln(s)$ should be a periodic function around a constant value. So, in this case one has

$$\frac{\partial \ln(n_s)}{\partial \ln(s)} = \tau + \theta[\ln(s)], \tag{23}$$

where $\theta(x)$ is a periodic function. Then, after integration one gets

$$n_s = Cs^\tau \exp^{\theta^*[\ln(s)]}, \tag{24}$$

where C is a constant and $\theta(x)^*$ is a periodic function such that $\partial\theta^*[\ln(s)]/\partial \ln(s) = \theta[\ln(s)]$. Now, by using Eq. (24) and following the same method as in the case of the rms width, it is easy to find that

$$\lambda_{n_s} = \tau\lambda_s. \tag{25}$$

Table II summarizes the values of the different logarithmic periods obtained for the BD model on $SC_x(3,5,5)$ substrates $(x=a,b,c)$. The results were obtained by fitting the data shown in the insets of Figs. 12, 14, and 15, with the aid of Eq. (14) for $N=2$. In the case of the BD model on $SC_a(3,5,5)$ fractals, the data exhibit some fluctuations and it is no longer possible to determine a reliable value of λ_{w_s}. The same shortcoming is found when attempting the evaluation of λ_{h_s} for the case of the $SC_c(3,5,5)$ substrate. In order to overcome this shortcoming, it should be necessary to perform the simulations on fractals with $k \gg 6$, but this task is very CPU-time demanding, so it is beyond our computational capabilities.

It is worth mentioning that all determined logarithmic periods can be compared to scaling relationships also involving exponents determined independently. In fact, the values of λ_{w_s} (column 2) are compared to $\ln(l)$ (column 3), as it follows from Eq. (18), obtaining an excellent agreement. Also, according to Eq. (17), the period λ_s (column 4) can be compared with the quotient given by $\lambda_{w_s}/\nu_\perp$ (column 5), where the exponent $\nu_\perp$ is taken from Table I, leading to an excellent agreement. On the other hand, the period λ_{h_s} (column 6) can be compared with the relationships given by Eqs. (22) (column 7) and (21) (column 8), where the exponents z and $\nu_\parallel$ are taken from Table I, obtaining agreement within error bars. Finally, the relationship $\lambda_{h_{ns}} = \tau\lambda_s$ given by Eq. (25), can be verified by comparing columns 9 and 10, also observing agreement within error bars.

Finally, we would like to comment that for growing aggregates in d-dimensional homogeneous media, one expects that the average volume of the frozen trees of size s (v_s), will scale according to [24]

$$v_s \propto h_s w_s^{d-1} \propto s^{\nu_\parallel + (d-1)\nu_\perp}, \tag{26}$$

so that one can define $v_s \propto s^\pi$, where π is an exponent. In previous work we showed that for ballistic aggregates in $1 \leqslant d \leqslant 5$ one has that $\pi \simeq 1$, indicating that the trees are compact structures [24]. By using this procedure, we determined $\pi = 1.05(2)$, $1.06(2)$, and $1.07(2)$ for the fractals of type a, b, and c (see Fig. 1), respectively. Since we evaluate the statistical error only, these exponents could be considered as pre-

TABLE II. List of the logarithmic periods obtained by fitting the log-periodic modulations of the power laws describing the internal structure of ballistic aggregates on different fractals. The data are also compared to scaling relationships that are explained in the text.

Fractal	λ_{w_s}	$\ln(l)$	λ_s	$\lambda_{w_s}/\nu_\perp$	λ_{h_s}	$z\ln(l)$	$\nu_\parallel\lambda_s$	λ_{n_s}	$\tau\lambda_s$
$SC_a(3,5,5)$	—	1.0986	3.4(1)	—	1.80(8)	1.75(6)	1.84(6)	4.8(2)	5.0(2)
$SC_b(3,5,5)$	1.10(3)	1.0986	3.2(1)	3.2(1)	1.70(8)	1.76(6)	1.77(6)	4.7(2)	4.7(2)
$SC_c(3,5,5)$	1.10(3)	1.0986	3.3(1)	3.2(1)	—	1.77(6)	1.84(6)	4.7(2)	4.9(2)

liminary evidence that frozen trees are also compact for ballistic aggregates in fractal media.

VII. CONCLUSIONS

We studied the ballistic deposition growth model in deterministic fractal substrates, embedded in $d=2$ dimensions, by means of numerical simulations, analyzing the data according to well-established scaling theories.

While the standard Family-Vicsek scaling approach seems to hold at least qualitatively, i.e., the interface width exhibits an initial power-law increase followed by saturation, systematic deviations from the expectation $W_{sat}(L) \propto L^{\alpha}$ are observed for large L values. In fact, the measured values of the interface width are larger than the scaling predictions, suggesting that the standard scaling approach has to be modified in order to properly describe the behavior of the interface upon growth on fractal media. Anyway, the obtained (effective) scaling exponents α, β, and z, interpolate between the already known values corresponding to $d=1$ and $d=2$ Euclidean dimensions. Furthermore, the relationship $z=\alpha/\beta$ holds, within error bars, and the determined dynamic exponent z is in reasonable agreement with subsequent independent measurements, performed by studying the internal structure of the aggregates (see, e.g., Table I).

On the other hand, the study of the properties of the internal structure of the aggregates, in terms of scaling laws describing the properties of frozen trees, i.e., branched structures that are inhibited for further growth due to shadowing effects and lie below the interface, provides an interesting and rich physical behavior. In fact, the standard scaling theory applied to the deposition on substrates of integer dimension predicts the power-law behavior of relevant physical observables as a function of the size of the trees, such as the rms width and height of the trees, as well as for the tree-size distribution. However, for fractal media with $d_f = \ln(5)/\ln(3)$ and $d_f=\ln(3)/\ln(2)$, we show that these power laws become modulated by soft log-periodic oscillations. These oscillations reflect the interplay between the spatial discrete scale invariance (DSI) of the underlying fractal substrates and the growing process. While it is well known that dynamic observables become coupled to the *spatial* DSI given time DSI [15–17], growing aggregates in fractal media provide a richer scenario. On the one hand, the rms width of the frozen trees, i.e., an intrinsically spatial observable measured along the direction parallel to the substrate, exhibits spatial DSI with the same fundamental scaling ratio $[\ln \lambda_{w_s} = \ln(l)]$ as that of the fractal. On the other hand, the rms height of the frozen trees, which is measured along the growing (time) direction perpendicular to the substrate, exhibits time DSI and its fundamental scaling ratio $(\ln \lambda_{h_s})$ is coupled to $\ln \lambda_{w_s}$ through the dynamic exponent z [see Eq. (22)], which is the realization of the more general relationship, also valid for any dynamic observable, given by Eq. (10). Of course, the size distribution of the frozen trees also exhibits DSI, which in a subtle way involves both spatial and time DSI, since it is an observable that depends on the structure of the trees developed along the directions parallel and perpendicular to the substrate.

We hope that this work will contribute to the understanding of growing aggregates in fractal media, also stimulating theoretical work aimed to describe the interplay between the underlying symmetries of the substrates and the behavior of physical observables characteristic of the processes occurring in those media.

ACKNOWLEDGMENTS

This work was financially supported by CONICET, UNLP, and ANPCyT (Argentina).

[1] A. L. Barabasi and H. E. Stanley, *Fractal Concepts in Surface Growth* (Cambridge University Press, Cambridge, 1995).
[2] *Kinetic of Aggregation and Gelation*, edited by F. Family and D. Landau (North-Holland, Amsterdam, 1984).
[3] *Fractals and Disordered Systems*, edited by A. Bunde and S. Havlin (Springer-Verlag, Berlin, 1992), p. 229.
[4] F. Family, in *Rough Surfaces: Scaling Theory and Universality*, edited by R. Jullien, L. Peliti, R. Rammal, and N. Boccara, Springer Proceedings in Physics Vol. 32 (Springer-Verlag, Berlin, 1988), p 193.
[5] J. S. Langer, Rev. Mod. Phys. **52**, 1 (1980), and references therein.
[6] E. Ben-Jacob, O. Schochet, A. Tenenbaum, I. Cohen, A. Czirók, and T. Vicsek, Nature (London) **368**, 46 (1994).
[7] S. Clar, B. Drossel, and F. Schwabl, J. Phys.: Condens. Matter **8**, 6803 (1996).
[8] E. V. Albano, R. C. Salvarezza, L. Vázquez, and A. J. Arvia, Phys. Rev. B **59**, 7354 (1999).
[9] F. Family, J. Phys. A **19**, L441 (1986).
[10] F. Family and T. Vicsek, J. Phys. A **18**, L75 (1985).
[11] M. J. Vold, J. Colloid Sci. **14**, 168 (1959); J. Phys. Chem. **63**, 1608 (1959); **64**, 1616 (1960).
[12] M. Kardar, G. Parisi, and Y.-C. Zhang, Phys. Rev. Lett. **56**, 889 (1986).
[13] B. Kutnjak-Urbanc, S. Zapperi, S. Milošević, and H. E. Stanley, Phys. Rev. E **54**, 272 (1996).
[14] D. Bessis, J. S. Geronimo, and P. Moussa, J. Phys. (Paris), Lett. **44**, 977 (1983); L. Pietronero, in *Order and Chaos in Nonlinear Physical Systems*, edited by S. Lundqvist, N. H. March, and M. Tosi (Plenum Publishing Corporation, New York, 1988).
[15] M. A. Bab, G. Fabricius, and E. V. Albano, Phys. Rev. E **71**, 036139 (2005).
[16] M. A. Bab, G. Fabricius, and E. V. Albano, Phys. Rev. E **74**, 041123 (2006).
[17] M. A. Bab, G. Fabricius, and E. V. Albano, Europhys. Lett. **81**, 10003 (2008).
[18] Didier Sornette, *Chaos, Fractals, Self-Organization and Disorder: Concepts and Tools*, 2nd ed. (Springer, New York, 2004).

[19] Didier Sornette, *Why Stock Markets Crash: Critical Events in Complex Financial Systems* (Princeton University Press, Princeton, New Jersey, 2003).
[20] Z. Rácz and T. Vicsek, Phys. Rev. Lett. **51**, 2382 (1983).
[21] P. Meakin, Phys. Rev. B **30**, 4207 (1984).
[22] M. Matsushita, Y. Hayakawa, and Y. Sawada, Phys. Rev. A **32**, 3814 (1985).
[23] P. Meakin, J. Phys. A **20**, L1113 (1987).
[24] F. Romá, C. M. Horowitz, and E. V. Albano, Phys. Rev. E **66**, 066115 (2002).
[25] C. M. Horowitz, M. A. Pasquale, E. V. Albano, and A. J. Arvia, Phys. Rev. B **70**, 033406 (2004).
[26] M. Matsushita and P. Meakin, Phys. Rev. A **37**, 3645 (1988).
[27] J. Krug and P. Meakin, Phys. Rev. A **40**, 2064 (1989).
[28] D. Sornette, Phys. Rep. **297**, 239 (1998).
[29] C. Castellano, M. Marsili, and L. Pietronero, Phys. Rev. Lett. **80**, 3527 (1998).
[30] A. Bunde and S. Havlin, in *A Brief Introduction to Fractal Geometry*, edited by A. Bunde and S. Havlin, Fractals in Science (Springer Verlag, Berlin, 1995), p. 1.
[31] R. F. S. Andrade, Phys. Rev. E **61**, 7196 (2000).